euspen's 24th International Conference & Exhibition, Dublin, IE, June 2024
www.euspen.eu

Frequency domain optimization of the tracking performance of a piezo actuator using reset control

Marvin Hakvoort[1,2], Christopher Mock[2], S. Hassan HosseinNia[1]

[1]*Department of Precision and Microsystems Engineering; Delft University of Technology, Mekelweg 2, 2628 CD Delft, The Netherlands*
[2]*Physik Instrumente (PI) GmbH &. Co. KG., Auf der Römerstraße 1, 76228 Karlsruhe, Germany*

m.hakvoort@student.utwente.nl; s.h.hosseinniakani@tudelft.nl;

Abstract

Customer demands for piezo positioning systems focus on higher closed-loop bandwidths and increased precision. However, poorly damped resonance frequencies often limit achievable bandwidths. Linear control limitations, such as Bode's gain-phase relation and the waterbed effect, constrain controller performance. Recent research suggests that nonlinear control methods, like reset control, can overcome these limitations. The "Constant in Gain – Lead in Phase (CgLp)" structure offers a lead in phase without sacrificing gain, unlike its linear counterpart. This work aims to leverage this property to improve closed-loop bandwidth, steady-state tracking, and disturbance rejection while maintaining the transient properties of the systems.
The controllers have been implemented and tested on a one-degree-of-freedom precision positioning stage with multiple dominant resonance frequencies. The CgLp element is used as an extension to the linear control structure in series with a proportional-integral (PI) tracking controller. To dampen the first dominant resonance frequency, a Positive Position Feedback (PPF) controller has been used in the inner loop. The controllers have been optimized solely based on the describing function (DF) analysis of the system using a Particle Swarm Optimization (PSO) algorithm. It has been shown that when properly setting the CgLp parameters, the effect of higher-order harmonics introduced by the resets is negligible, and the first-order DF approximation delivers an accurate frequency domain analysis. The results have shown that by using the additional CgLp element-based structure, the closed-loop bandwidth could be improved by 60%, and the overshoot could be kept below 5%. Additionally, steady-state tracking performance and disturbance rejection capabilities could be significantly improved.

1. Introduction

The current customer demands for nanopositioning systems such as piezo actuators go towards even higher closed loop bandwidths, increased precision and disturbance rejection capabilities. However, the maximum achievable bandwidths of these systems are often limited by one or multiple poorly damped resonance frequencies. The maximum achievable closed loop bandwidth of these systems is typically below the value of the first resonance frequency [1]. Additionally, fundamental limitations of linear control such as Bode's gain phase relation and the waterbed effect limit the achievable performance of these controllers.

Recent work has shown that nonlinear control strategies such as reset control can be used to overcome these limitations and improve the tracking performance of these systems [2]. Two of the most promising reset elements are called "Constant in gain – Lead in phase (CgLp)" and "Continuous Reset – Constant in gain – Lead in phase (CRCgLp)" and are typically used as an addition to a linear tracking controller [3]. In contrast to linear controllers, these elements are able to provide a lead in phase while having an almost constant gain. With linear controllers, Bode's phase gain relation for minimum phase systems states that a lead in phase always coincides with an increase in gain. Hence, if the robustness of the system has to be improved by for instance adding phase in the crossover region using a lead element, that also comes along with a decreased slope of the loop gain at the crossover frequency. This is not desired since a high gain at low frequencies and low gain at high frequencies with a steep crossover is desired for a proper tracking performance, according to the loop shaping constraints. With the previously mentioned CgLp and CRCgLp elements, this increase in gain can be avoided. Therefore, this additional phase can be used to either increase the phase margin of the system while maintaining a similar tracking performance or to increase the loop gain of the system compared to the linear case without affecting the stability margins according to the describing function (DF) analysis.

There are various methods for analyzing reset control systems or in general nonlinear controllers in the frequency domain. However, to make them an appropiate choice for industrial applications, the tuning and optimization process should be intuitive and take as little time as possible. One of the most well known methods is DF analysis of the reset control system which is based on the first order Fourier series expansion of the elements output [4]. Even though higher order harmonics of the signal are neglected with this approach, it can deliver an accurate estimation of the performance of the system, when it is ensured that these higher order harmonics are low enough in magnitude. This paper validates this approach using a single degree of freedom nanopositioning system. The CgLp and CRCgLp element based control structures are adjusted manually to ensure that the mentioned higher order harmonics are low enough in magnitude and the remaining parts of the linear control structure is optimized using the closed loop frequency response of the system. For a fair comparison, the reset controller based structures are also compared to the optimized linear controllers in terms of closed loop bandwidth, steady-state tracking performance and disturbance rejection capabilities.

Section 2 of this paper introduces the reset control fundamentals including an overview of the CgLp and CRCgLp elements. In section 3, the linear control structure is introduced. The tuning and optimization procedure as well as the results are shown and compared in section 4. Finally, section 5 concludes the paper and gives recommendations for future work.

2. Reset Control

This section introduces the relevant reset control essentials ranging from the basic state-space description of the reset controllers to the relevant frequency domain analysis tools. The general state-space description of the most basic reset element is given by [4]:

$$\begin{cases} \dot{\overrightarrow{x_\mathrm{r}}}(t) = \boldsymbol{A}_\mathrm{r}\overrightarrow{x_\mathrm{r}}(t) + \boldsymbol{B}_\mathrm{r}e(t) & \text{if } e(t) \neq 0 \\ \overrightarrow{x_\mathrm{r}}(t^+) = \boldsymbol{A}_\rho\overrightarrow{x_\mathrm{r}}(t) & \text{if } e(t) = 0 \\ u(t) = \boldsymbol{C}_\mathrm{r}\overrightarrow{x_\mathrm{r}}(t) + \boldsymbol{D}_\mathrm{r}e(t), \end{cases}$$

where $\boldsymbol{A}_\mathrm{r}$, $\boldsymbol{B}_\mathrm{r}$, $\boldsymbol{C}_\mathrm{r}$ and $\boldsymbol{D}_\mathrm{r}$ are the base-linear state-space matrices of the reset control system and $\boldsymbol{A}_\rho$ is the so called reset matrix which determines the portion of reset and is given by:

$$\boldsymbol{A}_\rho = \begin{bmatrix} \boldsymbol{A}_{\rho_\mathrm{r}} & \boldsymbol{0} \\ \boldsymbol{0} & \boldsymbol{I} \end{bmatrix},$$

with $\boldsymbol{A}_{\rho_\mathrm{r}} = diag(\gamma_1, \gamma_2, \dots, \gamma_{n_r})$ and $\gamma_i \in [-1, 1]$ being the resetting part of the reset matrix. The identity matrix can hence be used for states that should not reset. When looking at the state-space description above, it can be seen that a γ-value of zero represents a full reset of the state and that negative values even negate the states.

In figure 1, the output of this general reset element is shown as well as the first order Describing Function. Here, the clear advantage of the reset control element can be seen by taking a look at the phase difference between the input and output signal, which in this case is in fact only -38° instead of the -90° of the standard linear integrator.

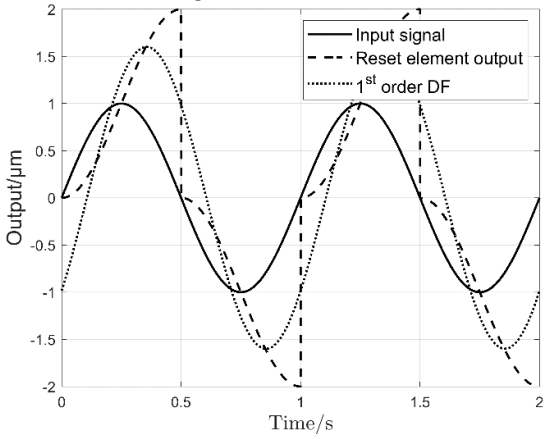

Figure 1. Output of a general reset element and the 1st order Describing Function of the output

The set of equations to analytically calculate the first order describing function and the higher order harmonics of the output is given in [4]. As already mentioned, these higher order harmonics are generally not desired, especially in the low frequency region. There are also other methods for analyzing reset control systems in the frequency domain such as the so called pseudo-sensitivity method [2]. Whereas these methods are considered to be more accurate than the DF-based analysis, the calcution requires significantly more time and hence limits their industrial applicability. In addition to that, the reset control system can be designed such that the DF-based analysis delivers an accurate estimation of the frequency response.

To make use of the phase advantages of the reset controller only in the appropiate frequency range, which is typically the open loop crossover region, the CgLp and CRCgLp elements have been introduced.

An overview of the CgLp and CRCgLp elements can be seen in figure 2.

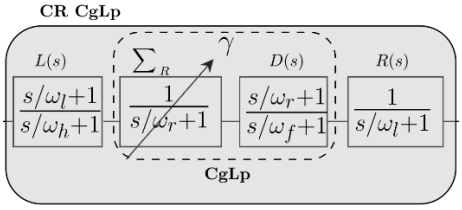

Figure 2. Structure of the CgLp and CRCgLp elements [3] (The arrow indicates the output of the filter reset to γ)

The CgLp element consists of a so called "First order reset element (FORE)" [5] which is essentially the nonlinear equivalent of a linear first order lowpass filter [4]. Similar to the previously introduced reset integrator, this element shows a reduced phase lag. In addition to that, a lead filter is located behind this FORE element. The advantage of this combination is that the gains of these elements almost exactly cancel but due to the reduced phase lag, a total lead in phase is obtained, which can not be achieved with linear controllers. The CRCgLp element contains an additional lead filter in front of the CgLp element and a lag filter behind it. Due to the lag filter behind the reset element, the influence of the higher order harmonics can be reduced compared the CgLp element. In addition to that, the lead filter changes the reset condition to [4]:

$$\frac{\dot{e}(t)}{\omega_\mathrm{l}} + e(t) = 0$$

The lead and lag filters do not influence the DF of the open loop if $\omega_h \gg \omega_\mathrm{r}$ and $\omega_h \gg \omega_\mathrm{c}$. Another interesting property of this lead element is that a reduction of the ratio $\omega_\mathrm{l}/\omega_\mathrm{c}$ decreases the overshoot of the system, which can be used to optimize the transient response of the system. However, a reduction of this ratio also leads to a longer settling time.

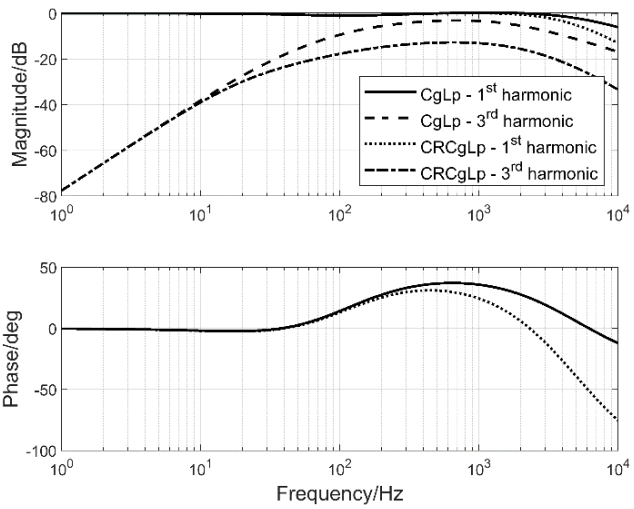

Figure 3. High Order Sinusoidal Inout Describing function (HOSIDF) comparison between a CgLp and CRCgLp element.

Figure 3 shows the frequency response of the 1st and 3rd order harmonics of an example CgLp and CRCgLp element. The constant gain of the two elements can clearly be seen up until a frequency which is far above the desired control bandwidth. Similarly, the additional phase lead of the elements is visible which starts approximately at the frequency ω_r. When taking a look at the magnitude of the 3rd order harmonics, it can be seen

that the magnitude is significantly lower for the CRCgLp element due to the additional lag filter after the CgLp element.

3. Linear control structure

As already mentioned before, the CgLp and CRCgLp structures are typically used as an addition to the linear control structure. For the tracking controller, a proportional-integral (PI) controller has been used with an integrator cut-off well before the crossover frequency. This prevents the phase lag of the integrator from influencing the phase in the crossover region.

To effectively attenuate the resonance frequency of the system, an active damping control scheme has been implemented. Therefore, a Positive Position Feedback (PPF) controller has been used, which is given by [6]:

$$C_{\mathrm{ppf}}(s) = \frac{\Gamma}{s^2 + 2\zeta_{\mathrm{d}}\omega_{\mathrm{d}}s + \omega_{\mathrm{d}}^2}$$

where Γ is the gain of the PPF controller, ζ_{d} the damping ratio and ω_{d} is cut-off frequency. An overview of the complete control scheme can be seen in figure 4.

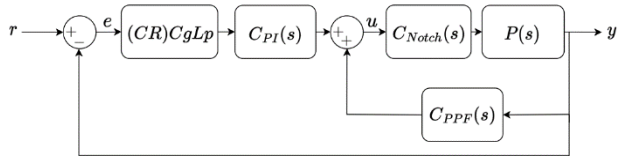

Figure 4. Overview of the control structure.

During initial optimizations it has been observed that the PPF damping controller was not sufficient to effectively dampen higher frequency resonance modes. Hence, a notch filter has been used in the inner loop as well.

4. Results

The results obtained with a single degree of freedom piezo actuator will be shown in this section. This includes an introduction to the system as well as the optimization algorithm that has been used to tune the controllers.

4.1. Plant model

The piezo actuator that has been used in this work has multiple weakly damped resonance frequencies ranging from 125 Hz to 350 Hz. The frequency response measurement (solid line) as well as the frequency response of an identified model of the system (dashed line) can be seen in figure 5.

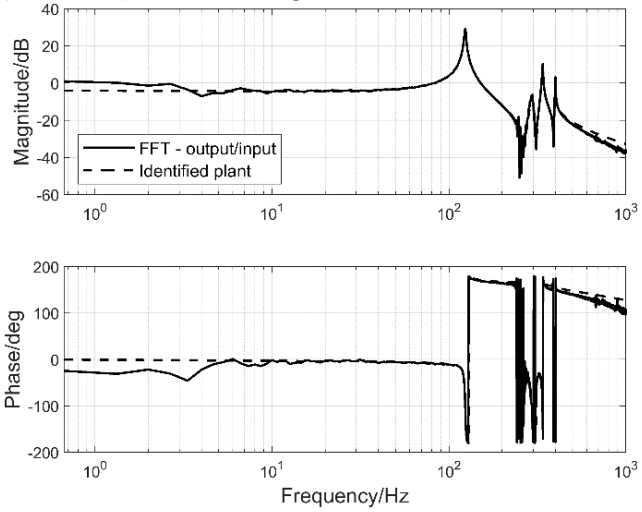

Figure 5. Frequency response of the measured and identified system

4.2. Optimization algorithm

To optimize the control structure in the frequency domain, a Particle Swarm Optimization (PSO) algorithm has been used [7]. The cost function that has been used is based on the closed loop frequency response of the system and is given by:

$$J_{\mathrm{T}} = \int_{\omega_{\min}}^{\omega_{\max}} W(\omega)\big||T(j\omega)| - |T_{\mathrm{ideal}}(j\omega)|\big|d\omega$$

where $T(j\omega)$ is the complementary sensitivity function obtained with the parameter set and $T_{\mathrm{ideal}}(j\omega)$ is a targeted closed loop frequency response that is set beforehand. The frequency dependent weighting function $W(\omega)$ has been set to:

$$W(\omega) = \frac{1}{\sqrt[4]{\omega}}$$

to ensure that low frequency deviations of the complementary sensitivity function are penalized more than high frequency ones.

Furthermore, a constraint for the sensitivity function has been implemented which is essentially just an upper limit for the sensitivities. Since the peak sensitivity is a measure for the robustness of the system, this parameter could be adjusted according to the desired robustness properties of the system. In this work a peak sensitivity of 3.5 dB has been used.

To evaluate the stability of the systems during the optimizations, the so-called Nyquist Stability Vector [8] has been used. To reduce the required time for the optimization, the stability has been checked first, such that the cost function has only been evaluated for stable systems.

4.3. Measurement results

For a fair comparison, the control structure which is solely based on the linear PI and PPF controllers is optimized as well using the PSO algorithm. To evaluate the performance of the optimized controllers in terms of closed loop bandwidth, steady-state tracking performance and disturbance rejection capabilities, the system has been excited by sinusoidal inputs for frequencies between 1 Hz and 1 kHz and the steady-state inputs and outputs have been recorded. To ensure that the higher order harmonics introduced by the reset controller are significantly lower in magnitude than the first harmonic, such that the DF analysis delivers an accurate analysis of the frequency response, the reset control parameters have been fixed and tuned prior to the optimization. Since it could be expected that higher open loop crossover frequencies can be achieved with the CgLp and CRCgLp elements, ω_r has been set to 100 Hz, which is slightly larger than the achievable crossover for the linear control structure only. This frequency determines the start of the phase lead which is desirable in the crossover region of the system. The reset parameter has been set to $\gamma = 0.4$ for the CgLp element and $\gamma = 0.15$ for the CRCgLp. The lower value for the CRCgLp element is possible since higher order harmonics are further reduced to the additional lag filter behind the CgLp element. The two taming pole frequencies have been set to $\omega_f = \omega_h = 2\pi/(10T_{\mathrm{s}})$ such that they do not interfere with the relevant dynamics. The cut-off frequency of the lead and lag filter ω_l when using the CRCgLp element has been set to 60 Hz. Hence, the only parameters left to optimize using the PSO algorithm were the PI control and PPF controller parameters: Γ, $\zeta_{\mathrm{d}}, \omega_{\mathrm{d}}, k_{\mathrm{p}}$ and ω_{i}.

Figure 6 shows the closed loop response comparison of the steady-state outputs of the systems for the linear controllers only (PI-PPF) and the CgLp and CRCgLp controller-based structures. The CgLp and CRCgLp controllers significantly outperform the linear control structure in terms of the achieved closed loop bandwidths of the systems.

In figure 7 the steady-state peak to peak error values for the chosen frequency range is shown for the three control structures which is essentially the sensitivity response of the systems. The lower sensitivity in the low frequency region indicates a superior steady-state tracking performance of the CgLp and CRCgLp based control structures compared to the linear structure. This is due to the higher loop gains that could be achieved because of the additional phase the reset elements can provide. The higher loop gains also indicate an improved disturbance rejection capability of the reset controller-based systems.

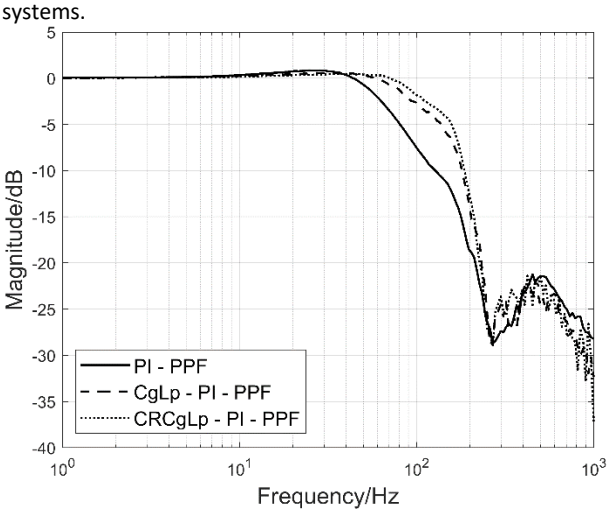

Figure 6. Closed loop frequency response of the three controllers.

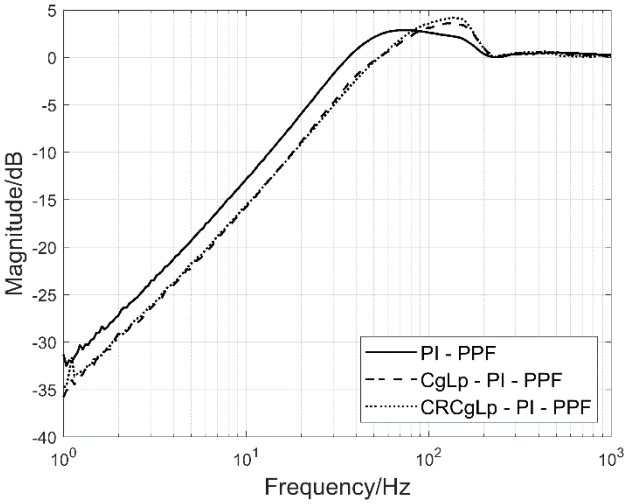

Figure 7. Sensitivity comparison of the three controllers.

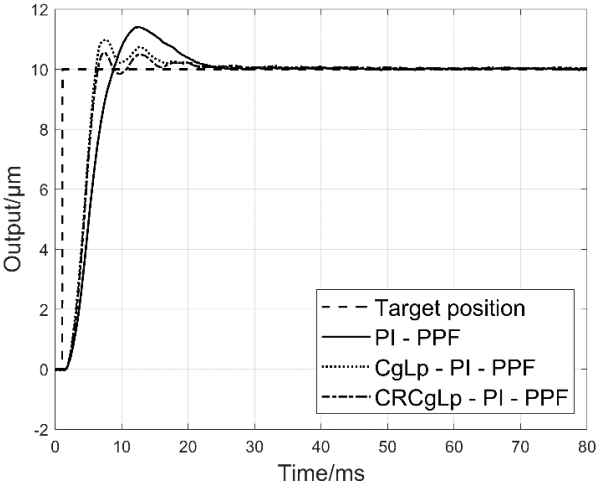

Figure 8. Step response comparison of the three controllers.

A step response comparison for the three control structures can be seen in figure 8. The higher loop gains and crossover frequencies of the two reset controller optimization results can clearly be seen in the reduced rise time of the response. In addition to that the overshoot of the CgLp and CRCgLp structures is reduced compared to the linear control structure only and could be reduced to 5 % for the CRCgLp based controller.

5. Conclusion

In this paper, a DF analysis based frequency domain optimization method has been investigated for the usage with a single degree of freedom nanopositioning stage. The reset control parameters have been tuned prior to the optimization process to ensure the exclusive use of the DF analysis of the system delivers an accurate estimation of the system's frequency response and to reduce the required time for time for the optimization algorithm to converge. The results have shown a significant improvement of the closed loop bandwidth, the steady-state tracking performance and disturbance rejection capabilities of the systems based on the CgLp and CRCgLp elements. The closed loop bandwidth of the system with the CRCgLp element has improved by 60 % and the overshoot in the step response was kept below 5 %.

Given the current customer demands of higher closed loop bandwidths and an improved steady-state tracking performance and disturbance rejection capabilities, linear control reaches its limits at some point. This paper has shown that reset control can help to overcome these limitations using a DF-based analysis of the system. Due to the optimization in the frequency domain, not much time is required for the algorithm to converge, which makes it a promising procedure for industrial usage. Further research could investigate an improvement of the linear control structure which does not require the usage of the additional notch filter. In addition to that, more intuitive design methods for the initial design of the linear controller could be developed.

References

[1] D. Russel, A. San-Millan, V.Feliu and S. S. Aphale, "Butterworth pattern-based simultanuous damping and tracking controller design for nanopositioning systems," 2015 European Control Conference (ECC), vol.2, 2016.

[2] A. A. Dastjerdi, K. Heinen, and S. H. HosseinNia, "A frequency-domain tuning method for a class of reset control systems," IEEE Access, vol.9, pp. 40950-40962, 2021.

[3] N. Karbasizadeh and S. H. HosseinNia, "Continuous reset element: Transient and steady-state analysis for precision motion systems," Control Engineering Practice, vol. 126, p. 105232, 2023.

[4] N. Saikumar, K. Heinen, and S. H. HosseinNia, „Loop-shaping for reset control systems," Control Engineering Practice, vol. 111, p. 104808, 2021.

[5] L Zaccarian, D Nesic, AR Teel, First order reset elements and the Clegg integrator revisited, Proceedings of the 2005, American Control Conference, 2005., 563-568

[6] R. Moon, A. San-Millan, M. Aleyaasin, V. Feliu, and S. Aphale, "Selection of positive position feedback controllers for damping and precision positioning applications," Communications in Computer and Information Science, pp. 289-301, 2017.

[7] J. M. Shashank, Nature-inspired optimization algorithms with Java: A look at optimization techniques. Apress, 2022.

[8] A. A. Dastjerdi, A. Astolfi, and S. H. HosseinNia, "Frequency-domain stability methods for reset control systems," Automatica, vol. 148, p. 110737, 2023.